Coherent Integration of Optical Flow for Track-Before-Detect Radar Detection

Lukas Herrmann*, Edmund Førland Brekke†, Egil Eide*
*Dept. Electronic Systems, Norwegian University of Science and Technology, Trondheim, Norway
†Dept. Engineering Cybernetics, Norwegian University of Science and Technology, Trondheim, Norway
Email: lukas.herrmann@ntnu.no; edmund.brekke@ntnu.no; egil.eide@ntnu.no

***Abstract*—The detection of small and dim targets under low signal-to-noise ratio (SNR) circumstances is a commonly encountered yet challenging endeavour in radar signal processing. The standard approach to deal with undesirable background conditions involves coherent processing and integration with subsequent detection directly applied to the radar signals. However, optical flow, a widespread visual tracking method, has rarely been used in this context. In this paper, we address the issue of radar target detection in low SNR scenarios by employing optical flow on radar images. This work focuses on the divergence of the optical flow vector field, utilising a novel approach of coherently integrating consecutive flow fields calculated against a homogeneous reference plane. The proposed methodology allows for more robust target identification and thus a precise initialisation of tracking systems. To validate and demonstrate the benefits of the proposed approach, simulations are conducted and discussed.**

***Index Terms*—radar, target detection, optical flow, dim targets, low signal-to-noise ratio, track-before-detect**

I. Introduction

Across numerous applications, the detection and tracking of targets form the core of every radar system and have been explored for decades [1]. However, it still remains difficult under particular circumstances. For example, in maritime situational awareness, challenges arise due to long ranges, small, manoeuvrable targets, and unfavourable, noisy backscatter from the surroundings. The small *radar cross section* (RCS) of such targets together with a high background noise level results in very low *signal-to-noise ratios* (SNRs) which makes it difficult to detect a target's presence.

Generally, there are two different types of detections in radar signal processing and target tracking. The first kind of detection is concerned with the extractions of (point-) measurements from radar signals which are then to be provided to a tracking method. This process is usually part of the radar signal processing chain [2]. The second kind is to make a detection decision whether a target is present or not based on the input measurements [3]. Conventionally, the extraction of measurements from a radar image (range-azimuth/range-Doppler) is done employing a *constant false alarm rate* (CFAR) detector, and variations of it, which is considered state of the art [1]. Contrary to the traditional approach of applying a threshold for the extraction of measurements, it is also possible to use the entire raw sensor image as input to make a decision about the presence or absence of a target. This is commonly referred to as *track-before-detect* (TBD) which is computationally more expensive, yet can potentially achieve superior performance for low SNR targets [4].

In camera-based visual tracking, the usage of optical flow, with its established methods such as the Lucas-Kanade, Horn-Schunck, and Farneback algorithms, and numerous variations is considered state of the art [5]. Unlike its use within the computer vision community, optical flow methods for radar signal processing have rarely been explored so far. There exist approaches, commonly used in automotive applications such as [6], [7], where radar and camera detection and tracking are combined, but usually the fusion is done at a later stage such that optical flow and its variations are solely applied to the camera part whereas radar signal processing is carried out separately. In meteorology, fore- and nowcasting have been done by means of weather radar together with optical flow analysis [8], [9]. In sonar tracking, for moderate SNRs, segmentation, motion estimation, and subsequent tracking based on optical flow has been done in [10]. In [11] visual tracking methods based on optical flow have been used for navigation in a maritime radar application. However, none of these methods deal with noisy raw radar data. To the best of the authors' knowledge, optical flow has not been used for radar-based target detection before. In general, the application of optical flow to noisy images is conceptually counterintuitive and comes with its limitations [12], [13].

In this work, however, we use a novel approach to deal with the detection of weak radar targets hidden in noise. As opposed to calculating the optical flow within consecutive frames, we calculate the optical flow for every frame concerning a homogeneous reference plane with unity intensity. This enables finding target features that are defined by the targets' *point spread function* (PSF) in the raw radar image even when embedded in heavy noise. Conceptually, this can be viewed as TBD as the final decision about a target presence is based on non-thresholded raw radar images as input and the coherent integration of the optical flow field.

The outline of the paper is as follows: Section II states the problem formulation and the proposed method's underlying

The authors would like to acknowledge the support provided by the Norwegian Research Council under SFI AutoShip (project number 309230), and the European Union's Horizon 2020 research and innovation program under the PERSEUS doctoral program (Marie Skłodowska-Curie grant agreement number 101034240).

model. Section III details our proposed solution while in Section IV its effectiveness is demonstrated and discussed based on simulation results. Finally, the paper is concluded in Section V together with some research prospects.

II. Problem Formulation

We consider a scenario where a sensor (e.g., a maritime radar), located at the centre of a coordinate frame, illuminates our region of interest. The radar provides two-dimensional position information which is typically obtained in polar coordinates (range-azimuth). To retain linearity, assumptions based on the radar resolution and polar to Cartesian transformations can be used [14]. For simplicity, it is assumed that the centre of each range-azimuth cell is converted to Cartesian coordinates. The measurements at discrete time $k = 1, ..., K$ are represented as an array of resolution cells (pixels) $\mathbf{z}_k = \left[z_k^{(1,1)}, ..., z_k^{(i,j)}, ..., z_k^{(I,J)}\right]$. The value of each cell (i, j) within the measurements represents the magnitude of the backscattered complex radar signal where $i = 1, ..., I$ and $j = 1, ..., J$ denote the number of cells in x- and y-direction, respectively, with I and J being the number of cells in each direction.

A. Target model

The measurement array $\mathbf{z}_k$ depends on the presence of targets and their kinematic state. At time k, the kinematic state of the m-th target, where $m = 1, ..., M$, is represented by its state vector $\mathbf{x}_k = [x_k \ \dot{x}_k \ y_k \ \dot{y}_k]^{\mathrm{T}}$ where x_k, y_k are the Cartesian coordinates of the target position and $\dot{x}_k$, $\dot{y}_k$ are the corresponding velocities. A target is assumed to transition according to a constant velocity model [14] with the transition density given by:

$$f(\mathbf{x}_k^m|\mathbf{x}_{k-1}^m) = \mathcal{N}(\mathbf{x}_k^m; \mathbf{F}\mathbf{x}_{k-1}^m, \mathbf{Q}) \ , \tag{1}$$

where

$$\mathbf{F} = \begin{bmatrix} 1 & T & 0 & 0 \\ 0 & 1 & 0 & 0 \\ 0 & 0 & 1 & T \\ 0 & 0 & 0 & 1 \end{bmatrix}, \mathbf{Q} = q \begin{bmatrix} \frac{1}{3}T^3 & \frac{1}{2}T^2 & 0 & 0 \\ \frac{1}{2}T^2 & T & 0 & 0 \\ 0 & 0 & \frac{1}{3}T^3 & \frac{1}{2}T^2 \\ 0 & 0 & \frac{1}{2}T^2 & T \end{bmatrix}, \tag{2}$$

with q being the process noise variance and T being the sampling period defined by the radar rotation rate.

B. Sensor model

The contribution of a target to the measurement image is defined by the physical appearance and orientation, the RCS, and the PSF. Within the sensor image, the energy of the target signal can be spread across multiple surrounding measurement cells. For simple point scatterers, the PSF $h(\mathbf{x}_k^m)$ is merely defined by the sensor and thus dependent on the resolution as well as the reception and processing process. We assume a Gaussian PSF, scaled such that the maximum value is unity, which is given by:

$$h(\mathbf{x}_k^m) = \exp\left(-\frac{(i - x_k^m)^2}{2\sigma_x^2} - \frac{(j - y_k^m)^2}{2\sigma_y^2}\right) , \tag{3}$$

where σ_x^2 and σ_y^2 determine the spread in x- and y- direction respectively. Thus, every measurement $z_k^{(i,j)}$ can be denoted as:

$$z_k^{(i,j)} = \begin{cases} \sum_{m=1}^{M} s_k^{(i,j),m} + w_k^{(i,j)}, & \text{if } \mathcal{H}_1 \text{ is true} \\ w_k^{(i,j)}, & \text{if } \mathcal{H}_0 \text{ is true} \end{cases} , \tag{4}$$

where $\mathcal{H}_1$ indicates the assumption that at least one target is present, and $\mathcal{H}_0$ indicates nuisance only. The signal part $s_k^{(i,j),m}$ is defined as:

$$s_k^{(i,j),m} = A_k^m h(\mathbf{x}_k^m) \tag{5}$$

with A_k^m being the maximum amplitude of a target return, defined as the magnitude of a complex radar signal $A_k^m = |\Gamma_k^m \cdot e^{j\varphi_k^m}|$ where Γ_k^m represents the effective reflectivity. The phase φ_k^m is assumed to be uniformly distributed over the interval $[0, 2\pi)$. The noise term $w_k^{(i,j)}$ in (4) is the magnitude of circularly symmetric complex Gaussian noise with zero mean and covariance σ_n^2 i.e., $w_k^{(i,j)} = |n_k^{(i,j)}|$ and hence $w_k^{(i,j)} \sim |\mathcal{N}_c(n_k^{(i,j)}; 0, \sigma_n^2)| = \text{Rayleigh}(w_k^{(i,j)}; \eta)$. This term is assumed to represent all present noise caused by both thermal noise and unwanted background reflections. Assuming complex Gaussian noise, resulting in a Rayleigh distributed noise envelope, is a commonly used assumption for radar sensors [1]. In the case when no target is present, the *probability density function* (PDF) of the measurements $z_k^{(i,j)}$ at each time step k, is therefore given by the Rayleigh distribution:

$$p_0(z_k^{(i,j)}|\mathcal{H}_0) = \frac{z_k^{(i,j)}}{\eta} \exp\left\{-\frac{(z_k^{(i,j)})^2}{2\eta}\right\} . \tag{6}$$

With a non-fluctuating (Swerling 0) target present in Rayleigh noise, the PDF for the measured amplitude in each cell changes to a Rician distribution:

$$p_1(z_k^{(i,j)}|\mathcal{H}_1) = \frac{z_k^{(i,j)}}{\eta} \exp\left\{-\frac{(z_k^{(i,j)})^2 + A_k^m h(\mathbf{x}_k^m)}{2\eta}\right\} \mathcal{I}_0\left(\frac{z_k^{(i,j)}\sqrt{A_k^m h(\mathbf{x}_k^m)}}{\eta}\right) , \tag{7}$$

where $\mathcal{I}_0$ is the modified Bessel function of order 0 [15], [16].

C. Detection

In order to detect a target, the Neyman-Pearson lemma [17] asserts that the test achieving the maximum probability of detection P_D subject to a maximum probability of false alarm P_{FA} is the likelihood ratio test:

$$\mathcal{L} = \frac{p_1}{p_0} \underset{\mathcal{H}_0}{\overset{\mathcal{H}_1}{\gtrless}} t \ , \tag{8}$$

where $\mathcal{L}$ indicates the likelihood ratio and t is the threshold to be determined.

In practical applications, both p_0 and p_1 are usually not readily available. Even when assuming certain distributions the underlying parameters are unknown and may be time-varying. The parameters must therefore be estimated. A CFAR detector

estimates the background noise in each cell as a function of a specified number of N surrounded auxiliary cells, which can be further used to set the threshold accordingly. The background power η is estimated by the *maximum likelihood estimator* (MLE) $\hat{\eta} = \sum_{n=1}^{N} \frac{1}{N} z^n$. As the MLE is random the CFAR detector applies a factor α to account for the uncertainty of $\hat{\eta}$. For Rayleigh background noise, this factor is given by:

$$\alpha = \sqrt{N\left(P_{FA}^{-\frac{1}{N}} - 1\right)}\,, \tag{9}$$

where N is the number of auxiliary cells and P_{FA} is the desired probability of false alarm. Since the noise power is the maximum likelihood estimate, the threshold obtained from the generalised likelihood ratio test is given by:

$$t = \sqrt{N\left(P_{FA}^{-\frac{1}{N}} - 1\right)}\,\hat{\eta}\,. \tag{10}$$

This detector is commonly known as the *cell-averaging* CFAR (CA-CFAR) detector and it is the detector we use in the remainder of this paper when referring to a CFAR detector [1].

III. Detection Based on Optical Flow

In this section, we are going to introduce our novel detection method for radar target detection based on optical flow.

Optical flow is a fundamental tool in computer vision for analysing motion within image sequences. The basic idea is to formulate a velocity describing how the intensity of every pixel changes from one timestep to the next. Though this is generally not solvable [12], various algorithms exist based on different assumptions. The Horn-Schunck method formulates optical flow estimation as a variational problem [18]. Define the intensity at a certain point x, y within the image plane at time t as $I(x, y, t)$. Assuming both brightness constancy and spatial smoothness, the method aims to minimise the energy functional that represents the error in the brightness constancy and smoothness constraints. The energy functional is given by:

$$E = \iint \left(I_x u + I_y v + I_t\right)^2 + \alpha^2 \left(|\nabla u|^2 + |\nabla v|^2\right) \mathrm{dxdy}\,, \tag{11}$$

where u, v represent the horizontal and vertical components of the optical flow vector field, and $I_x = \frac{\partial I}{\partial x}$, $I_y = \frac{\partial I}{\partial y}$, and $I_t = \frac{\partial I}{\partial t}$ denote the spatiotemporal derivatives of the image intensity I with respect to the image coordinates x, y, and time t, respectively. Furthermore, the spatial gradients are denoted by ∇, and α is the regularisation parameter of the smoothness constraint [18].

The resulting system of partial differential equations is solved iteratively for a pixel i, j of a frame at a discrete time step k to obtain the optical flow [19]:

$$u_{(i,j)}^{p+1} = \bar{u}_{(i,j)}^{p} - \frac{I_i(I_i\bar{u}_{(i,j)}^{p} + I_j\bar{v}_{(i,j)}^{p} + I_k)}{\alpha^2 + I_i^2 + I_j^2}\,, \tag{12}$$

$$v_{(i,j)}^{p+1} = \bar{v}_{(i,j)}^{p} - \frac{I_j(I_i\bar{u}_{(i,j)}^{p} + I_j\bar{v}_{(i,j)}^{p} + I_k)}{\alpha^2 + I_i^2 + I_j^2}\,, \tag{13}$$

where p explicitly denotes the iterations. In (12) and (13), I_i, I_j, and I_k are estimates for the partial brightness derivatives whereas $\bar{u}$, $\bar{v}$ are local averages of the flow which are given in [18], [19].

The term I_k in the optical flow equation represents the estimate of the temporal gradient of the image intensity. It quantifies how the pixel intensities change over time between consecutive frames in a discrete image sequence. The definition of I_k for a certain pixel is given as:

$$I_k = I(i, j, k) - I(i, j, k-1)\,. \tag{14}$$

A. Optical flow with a constant reference

Typically, optical flow methods are applied to a set of images to determine the optical flow along the given sequence by quantifying the motion of the pixels between two consecutive image frames. In the case of radar images in low SNR scenarios, the image data, this paper is concerned with, consists to a large extent of noise. Thus, optical flow methods fail to track any motion of brightness patterns [13], [20].

Therefore, in this paper, we use the novel approach to calculate the optical flow of every frame not concerning the previous one, but with respect to a homogeneous reference frame with constant brightness:

$$I_k = I(i, j, k) - I_{ref}\,. \tag{15}$$

In other words, I_k is the change in the pixel intensity between the current frame and the reference.

As pointed out by Horn and Schunck in [18], the relationship between the optical flow in the image plane and velocities in the three-dimensional world is not always obvious. Motion can also be perceived as a change in an image even though the object did not physically move, and conversely, a moving object can still have a constant brightness pattern. Therefore, calculating the optical flow of a radar image against the homogeneous reference plane enables one to find target structures even when hidden in heavy noise. Leveraging on the fact that the spread of the intensity of a target in the image plane is represented by its PSF, the target can be made apparent in the optical flow domain. The PSF, being a smooth and distributed intensity function, will have varying pixel intensities according to (15). Pixels closer to the centre of the PSF will have higher intensities, gradually decreasing away from the centre. Pixels in regions where the PSF intensity decreases, show optical flow vectors pointing away from the centre, indicating motion away from the higher-intensity region. In regions where both frames have constant and equal intensity, the optical flow vectors would ideally be zero, indicating no motion. The Gaussian shape of the PSF introduces a smooth flow pattern, with vectors diverging gradually based on the PSF. The change in intensity for pixels that solely represent noise, causes a random optical flow vector dependent on the change in brightness compared to the reference.

For illustration, a typical radar measurement $\mathbf{z}_k$ with one target present with an SNR of 0 dB is shown in Fig. 1 for both the target only (a) and the target plus noise case (b). In Fig. 2,

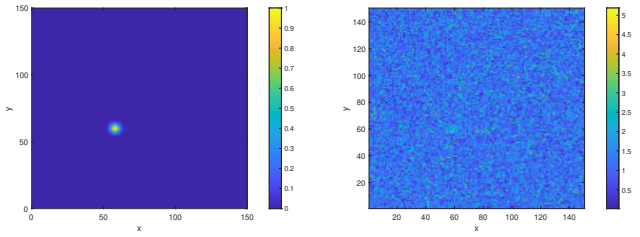

(a) Target only (b) Target + noise (0 dB)

Fig. 1: A single realisation of the measurement $\mathbf{z}_k$ at $k = 10$ with $\mathrm{SNR} = 0\,\mathrm{dB}$.

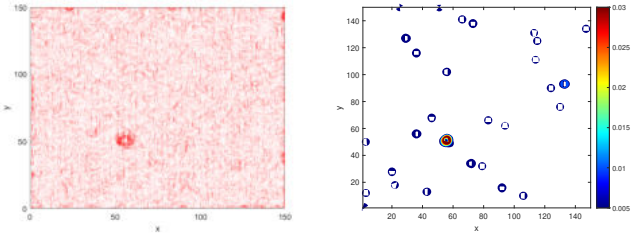

(a) Optical flow (b) Optical flow divergence

Fig. 2: Optical flow and its divergence for a measurement $\mathbf{z}_k$ at $k = 10$ with $\mathrm{SNR} = 0\,\mathrm{dB}$.

for the same measurement scenario, the optical flow vector field (a) and its divergence are shown. It can be seen that even though the target is hidden in heavy noise and in Fig. 1b it is visually nearly impossible to locate the target, it becomes a lot more obvious looking at the optical flow calculated against a homogeneous reference. As previously described, the spread of the target in the image plane causes the vector field to diverge. Thus, by calculating the divergence of the optical flow vector field, target-alike structures and noise can be further separated (cf. Fig. 2b). In most areas of the image, the divergence is zero, and at the target's location, the divergence is around three times higher than the divergence that is randomly created by the noise.

As optical flow constitutes a vector field, we can systematically integrate the vector field across multiple time intervals, aligning with the concept of TBD. Under the assumption of a target manoeuvring at a relatively slow pace compared to the sampling time, this further enhances the detection capabilities of the method. This is because the vectors representing the target accumulate coherently, while the flow vectors induced by noise aggregate randomly.

B. Implementation notes

The implementation of the proposed method is done as follows. For every time step, the optical flow of the raw radar image against the homogeneous reference is calculated as previously described. For the Horn-Schunck optical flow calculations the inbuilt MATLAB implementation *opticalFlowHS* [19] is used. Depending on the chosen integration time, the optical flow is coherently integrated over multiple time steps. The integration time has to be chosen under consideration of the target's reflectivity, motion, and acceptable time delays. Subsequently, the divergence of the integrated optical flow vector field is determined. For a detection decision to be made a threshold is applied to the obtained divergence. In this paper, we use a simple constant threshold as well as CFAR thresholding. Since the raw radar image is used as input, and more specifically since the thresholding is applied to the divergence of the optical flow vector field, the output after thresholding has to be clustered as the backscattered signal of a target can be spread over numerous resolution cells. We use *density-based spatial clustering of applications with noise* (DBSCAN) clustering as it does not require any prior knowledge about the number of clusters [21]. The output after clustering provides our detections whereby the centre position of each cluster is taken as the position of each obtained detection.

The whole signal processing chain is illustrated in Fig. 3.

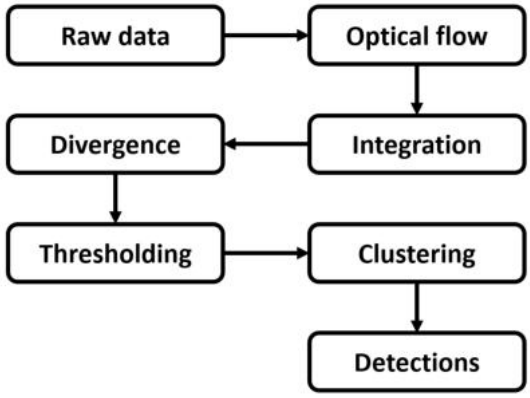

Fig. 3: Illustration of the proposed signal processing chain.

IV. Numerical Results

A. Simulation scenario

The simulation scenario consists of a single target, moving according to a nearly constant velocity model, observed by a maritime radar with a constant scan rate of $T = 1\,\mathrm{s}$ and $i = j = 150$ resolution cells in x- and y- direction, respectively. The process noise of the kinematic model is $q = 0.005$.

The target is assumed to be of a Swerling 0 type i.e., $A_k = A$. The target's mean power is set with respect to the indicated SNR values respectively and follows the relationship of the peak SNR:

$$\mathrm{SNR} = 10\ \log_{10}\left(\frac{A}{\eta}\right)\ , \tag{16}$$

where $\eta = 1$ is the noise power of the Rayleigh distributed noise defined in (6). The target is initially located at $[x\ y]^{\mathrm{T}} = [45\ 55]^{\mathrm{T}}$ with an initial velocity of 0.5 and 0.1 pixels per time step in x- and y- directions, respectively. In the simulation, the target's spread across the surrounded resolution cells is set to $\sigma_x^2 = \sigma_y^2 = 5$.

The MATLAB function for calculating the optical flow has been used with its default settings, meaning an expected smoothness of 1, a maximum number of iterations of 10, and a minimum absolute velocity difference of 0. For clustering after the thresholding step, DBSCAN has been used with a radius of one pixel and a minimum of one point within the radius, respectively, to form a cluster.

The CFAR thresholding has been done according to Section II-C, where the auxiliary cell number was set to $N = 15$ and the guard cell number was set to 5 which was chosen based on the expected target spread. The false alarm rate was set to $P_{FA} = 5 \cdot 10^{-5}$.

For the assessment and comparison of the different methods, the following definitions have been used. For the calculation of the probability of detection, a decision is counted as correct if the centre of a cluster is in the range of ± 3 pixels from the centre peak of the true target position. The probability of a false alarm is defined as the number of detection cells subtracted by the number of cells, that are according to the detection cluster belong to the target, divided by the total number of resolution cells in the image. These definitions are necessary to account for the fact that due to the target's spread, the intensity in more than one resolution cell can exceed the threshold, but still stem from the same target which is then addressed by clustering.

The results presented in the remainder of this section are obtained by averaging over 200 Monte Carlo trials.

B. Simulation results and discussion

The simulation results presented in Fig. 4 have been created by applying the previously explained proposed method to the data of the described simulation scenario. For thresholding the divergence of the optical flow, two different methods are shown. First, a simple constant threshold of 0.98 of the maximum value of the divergence of the optical flow vector field which is plotted in blue and referred to as COF-D-TH. Second, a CFAR threshold is applied to the divergence of the coherently integrated optical flow which is plotted in red and referred to as COF-D-CFAR. These are compared with a standard CFAR detection scheme i.e., a CFAR detector directly applied to the radar raw data. This is plotted in yellow and indicated as CFAR. The same clustering has been used for all of the methods. For a fair comparison, in the case of integration of the optical flow, the raw data has also been integrated over the same amount of time steps before performing CFAR detection. In dashed lines, the same is displayed for the results of using the measurements of just one time step without any integration.

As it can be seen from Fig. 4, for a constant probability of false alarm, the proposed method achieves the same detection performance for an SNR that is 2-2.5 dB lower. This holds for both cases, with and without integration. However, without coherent integration of optical flow, the proposed method is no longer really a track-before-detect method, and in addition, detection performance decreases. Generally, it is obvious that all methods perform better when integration is used which

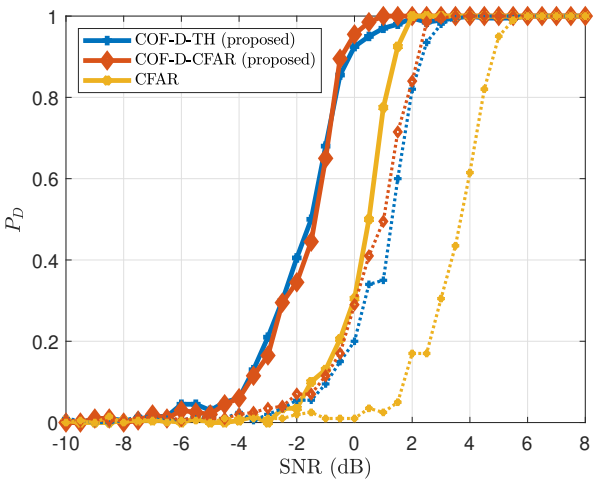

Fig. 4: Simulation results of the probability of detection P_D vs. the SNR averaged over 200 Monte Carlo runs with an integration interval of 5 frames (solid) and without integration (dotted) for a constant probability of false alarm of $P_{FA} = 5 \cdot 10^{-5}$.

was expected. Furthermore, it is worth noting that the simple constant threshold used in combination with the divergence of the optical flow gives almost similar results to the CFAR used on the same data. The advantages of a constant threshold are that it needs fewer resources in computation, and it can also easily be applied to the whole image. In contrast, the CFAR suffers from discontinuities at the edges which can potentially be problematic as targets are likely to appear at the edges of a surveillance area.

By looking at the amplitude histograms of the radar raw image and the divergence of the optical flow of one realisation at time step $k = 10$, shown in Fig. 5, we can further analyse how the proposed method works. By calculating the divergence of the optical flow, we transform our problem from the image domain to the optical flow domain. For the raw radar image (shown in 5a), the amplitudes seem to be Rayleigh distributed as the whole image is dominated by noise. For the shown $\mathrm{SNR} = 0\,\mathrm{dB}$ the target's amplitude distribution, with a maximum amplitude of $A = 1$ is clearly overwhelmed

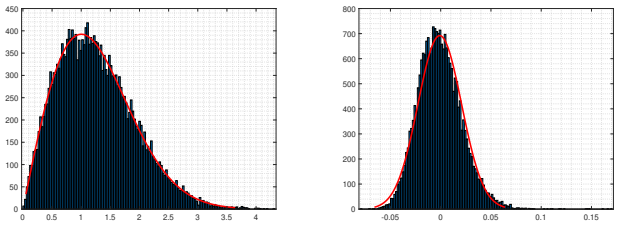

(a) Raw radar image (b) Optical flow divergence

Fig. 5: Amplitude histograms of one realisation of the raw radar image and the optical flow divergence ($\mathrm{SNR} = 0\,\mathrm{dB}$).

by the noise distribution. However, since only the target's characteristics in the radar image give rise to divergence in optical flow vector fields, the divergence is in most of the image part zeros or very close to it. The deviation around a divergence of zero which is caused by noise is normally distributed. The standard deviation is small compared to the divergence values that stem from the target's appearance which is around 0.15 in Fig. 5b. This is also the reason why a simple constant threshold produces such good results. The global noise distribution and the target distribution are well separated so that no local analysis is needed. In Fig. 5b, the standard deviation of the normal distribution is so low that the tail is already close to zero at divergence values caused by the target.

V. Conclusions and Future Directions

In this work, track-before-detect radar detection based on the coherent integration of optical flow was formulated and presented. Unlike conventional optical flow methods, mainly used in computer vision, the flow is not calculated for consecutive frames but for every single frame with respect to a homogeneous reference. It was shown that this causes divergence in the optical flow vector field due to the target's appearance even when hidden in heavy noise. Utilising this, a novel detection method was proposed. In simulations, the proposed approach was shown to have a considerably better detection performance for low SNRs when compared with a classical CFAR detector directly applied to radar raw data. It was further shown that the transformation from the image domain to the optical flow domain separates the target from noise sufficiently well that even a simple constant threshold can be used on the divergence of the optical flow to make a detection decision. Future work will be concerned with more detailed analyses, including (a) multi-target scenarios, (b) different clutter distributions (e.g., the K-distribution [22]) to represent more appropriate, application-specific conditions [23] as well as (c) implementations and testing on real data.

References

[1] M. A. Richards, *Fundamentals of Radar Signal Processing*. McGraw-Hill Education, Oct. 2005.

[2] M. A. Richards, J. Scheer, W. A. Holm, and W. L. Melvin, *Principles of modern radar*. SciTech Pub, 2010.

[3] S. Blackman, R. Popoli, and S. S. Blackman, *Design and Analysis of Modern Tracking Systems*. Norwood (MA): Artech House, 1999.

[4] M. Mallick, V. Krishnamurthy, and B.-N. Vo, *Integrated Tracking, Classification, and Sensor Management: Theory and Applications*. Hoboken (NJ): John Wiley & Sons Inc, 2013.

[5] D. Fortun, P. Bouthemy, and C. Kervrann, "Optical flow modeling and computation: a survey," *Computer Vision and Image Understanding*, vol. 134, p. 21, 2015.

[6] X. Tang, Z. Zhang, and Y. Qin, "On-Road Object Detection and Tracking Based on Radar and Vision Fusion: A Review," *IEEE Intelligent Transportation Systems Magazine*, vol. 14, no. 5, pp. 103–128, 2022.

[7] J. Bai, S. Li, L. Huang, and H. Chen, "Robust Detection and Tracking Method for Moving Object Based on Radar and Camera Data Fusion," *IEEE Sensors Journal*, vol. 21, no. 9, pp. 10761–10774, 2021.

[8] M. Peura and H. Hohti, "Optical flow in radar images," *European Conference on Radar in Meteorology and Hydrology (ERAD2004), Copernicus*, 2004.

[9] L. Mesin, "Short range tracking of rainy clouds by multi-image flow processing of X-band radar data," *EURASIP Journal on Advances in Signal Processing*, vol. 2011, no. 1, p. 67, 2011.

[10] D. Lane, M. Chantler, and Dongyong Dai, "Robust tracking of multiple objects in sector-scan sonar image sequences using optical flow motion estimation," *IEEE Journal of Oceanic Engineering*, vol. 23, no. 1, pp. 31–46, 1998.

[11] H. D. Flemmen, R. Mester, A. Stahl, T. H. Bryne, and E. F. Brekke, "Maritime radar odometry inspired by visual odometry," in *2023 26th International Conference on Information Fusion (FUSION)*, 2023.

[12] J. Barron, D. Fleet, S. Beauchemin, and T. Burkitt, "Performance of Optical Flow Techniques," in *IEEE Computer Society Conference on Computer Vision and Pattern Recognition*, 1992.

[13] F. Bergholm and S. Carlsson, "A "theory" of optical flow," *CVGIP: Image Understanding*, vol. 53, no. 2, pp. 171–188, 1991.

[14] Y. Bar-Shalom, X.-R. Li, and T. Kirubarajan, *Estimation with applications to tracking and navigation*. New York (NY): Wiley, 2001.

[15] Y. Boers, J. N. Driessen, F. Verschure, W. P. M. H. Heemels, and A. Juloski, "A Multi Target Track Before Detect Application," in *2003 Conference on Computer Vision and Pattern Recognition Workshop*, 2003.

[16] A. Lepoutre, O. Rabaste, and F. Le Gland, "Multitarget likelihood computation for track-before-detect applications with amplitude fluctuations of type swerling 0, 1, and 3," *IEEE Transactions on Aerospace and Electronic Systems*, vol. 52, no. 3, pp. 1089–1107, 2016.

[17] S. Kay, *Fundamentals of Statistical Signal Processing: Detection Theory*, vol. 1st ed. Upper Saddle River (NJ): Prentice-Hall, 1998.

[18] B. K. P. Horn and B. G. Schunck, "Determining optical flow," *Artificial Intelligence*, vol. 17, no. 1, pp. 185–203, 1981.

[19] "MATLAB - Object for estimating optical flow using Horn-Schunck method." https://se.mathworks.com/help/vision/ref/opticalflowhs.html.

[20] H. Spies and H. Scharr, "Accurate Optical Flow in Noisy Image Sequences," in *IEEE International Conference on Computer Vision (ICCV)*, 2001.

[21] M. Ester, H. Kriegel, J. Sander, and X. Xu, "A Density-Based Algorithm for Discovering Clusters in Large Spatial Databases with Noise," in *Proceedings of the Second International Conference on Knowledge Discovery and Data Mining*, 1996.

[22] K. Ward, R. Tough, and S. Watts, *Sea Clutter: Scattering, the K Distribution and Radar Performance*. IET Digital Library, 2013.

[23] D. Y. Kim, B. Ristic, X. Wang, L. Rosenberg, J. Williams, and S. Davey, "A Comparative Study of Track-Before-Detect Algorithms in Radar Sea Clutter," in *2019 International Radar Conference (RADAR)*, 2019.